

Clays and Clay Minerals, Vol. 49, No. 6, 000–000, 2001.

QUANTITATIVE X-RAY DIFFRACTION ANALYSIS OF CLAY-BEARING ROCKS FROM RANDOM PREPARATIONS

JAN ŚRODOŃ^{1,3*}, VICTOR A. DRITS^{2,3}, DOUGLAS K. MCCARTY³, JEAN C.C. HSIEH³ AND DENNIS D. EBERL⁴

¹ Permanent address: Institute of Geological Sciences PAN, Senacka 1, 31–002 Kraków, Poland

² Permanent address: Institute of Geology RAN, Pyzevskij 7, 109017 Moscow, Russia

³ Texaco Upstream Technology, 3901 Briarpark, Houston, TX 77042, USA

⁴ U.S. Geological Survey, 3215 Marine St., Boulder, CO 80303-1066, USA

Abstract—An internal standard X-ray diffraction (XRD) analysis technique permits reproducible and accurate calculation of the mineral contents of rocks, including the major clay mineral families: Fe-rich chlorites + berthierine, Mg-rich chlorites, Fe-rich dioctahedral 2:1 clays and micas, Al-rich dioctahedral 2:1 clays and micas, and kaolinites. A single XRD pattern from an air-dried random specimen is used. Clays are quantified from their 060 reflections, which are well-resolved and insensitive to structural defects. Zincite is used as the internal standard instead of rosendum, because its reflections are more conveniently located and stronger, allowing for a smaller amount of spike (10%). The grinding technique used produces powders free of grains coarser than 20 μm and suitable for obtaining random and rigid specimens.

Errors in accuracy are low, <2 wt % deviation from actual values for individual minerals, as tested on artificial shale mixtures. No normalization is applied and thus, for natural rocks, the analysis is tested by the departure of the sum of the measured components from 100%. Our approach compares favorably with other quantitative analysis techniques, including a Rietveld-based technique.

Key Words—Clay Minerals, Marls, Quantitative Analysis, Shales, X-ray Diffraction.

INTRODUCTION

X-ray powder diffraction is the best available technique for the identification and quantification of all minerals present in clay-rich rocks (claystones, mudstones, and marls). Accurate quantitative mineral analysis is important in petrological studies, engineering, and industrial applications of rocks that contain clay minerals. Whereas mineral identification is relatively simple and unambiguous if modern software and good mineral databases are available, accurate quantitative analysis of clays remains a formidable challenge (see reviews by Brindley, 1980; Reynolds, 1989; Snyder and Bish, 1989; McManus, 1991; Moore and Reynolds, 1997).

The main analytical difficulties in quantitative mineral analysis of rocks by X-ray diffraction (QXRD) are related to the chemical and structural characteristics of clay minerals: variable chemical composition, highly variable structures involving different patterns of layer interstratification including swelling interlayers, and various defects that disturb three-dimensional periodicity. These variations result in large differences in the intensities of XRD reflections between different specimens of the same mineral. Such variable intensities can result in large analytical errors in quantitative analysis if intensities are selected improperly. Thus, for natural rocks containing clays, techniques using whole-pattern fitting (Smith *et al.*, 1987) and sequential-pattern stripping (Batchelder and Cressey, 1998)

are difficult to apply. Rietveld refinement techniques (Bish and Howard, 1988; Taylor, 1991) face the same difficulty; clay structures are too complex to be modeled and refined for a routine quantitative analysis. Thus, instead of refining the patterns theoretically, a catalog of experimental patterns is used to quantify clays as in the whole-pattern fitting approach (SIROQUANT program: Taylor and Matulis, 1994, Ward *et al.*, 1999).

Whole-pattern methods do not take advantage of the fact that different classes of XRD reflections have very different sensitivity to chemical and structural variations, a phenomenon of particular importance for clay minerals (Moore and Reynolds, 1997, Chapter 10). In the present authors' opinion, the selection of insensitive analytical reflections offers a better chance for success, and that approach was used in this study.

Another major source of error in quantitative analysis of rocks containing clays is the platy habit of clay crystallites resulting in a tendency for preferred orientation. The degree of orientation of crystallites of the same mineral can vary by an order of magnitude between specimens prepared using the same technique and measurements of orientation are too tedious to be applied for routine analyses (Reynolds, 1989). For this reason, the clay minerals content in rocks often has not been measured accurately. Typically the proportions of the clay minerals in a clay size-fraction (*e.g.* <2 μm) are determined from oriented preparations, and relative variations within the clay group are studied (see review in McManus, 1991), which may be

* Corresponding Author

recalculated into percentages of the bulk rock (*e.g.* Lynch, 1997). Such normalization makes it impossible to judge the accuracy of the analysis by the departure from 100%. Furthermore, there is no reason to expect that the relative proportions of clays in a particular size-fraction are representative of the whole rock.

Application of an orienting internal standard (*e.g.* pyrophyllite: Mossman *et al.*, 1967) does not solve the problem because the degree of orientation of different minerals in the same specimen can be different and relative intensities depend on orientation (Reynolds, 1989). Orientation-related problems can be avoided by using a random preparation. Techniques for producing such preparations from clay-rich rocks have been described previously (Smith *et al.*, 1979; Moore and Reynolds, 1997; Hillier, 1999 and references therein).

Other sources of error in quantitative analyses are not specific to the nature of the clay minerals. Grinding and homogenization procedures are probably the most serious.

This study describes a procedure for quantitative analysis of rocks that contain clays by using random powders and diagnostic reflections that are insensitive, or have acceptably low sensitivity, to structural and chemical variations. Different sources of analytical error were evaluated systematically and an analytical procedure was optimized.

DERIVATION OF THE ANALYTICAL EQUATION

The internal standard technique (Klug and Alexander, 1974, p. 549) was selected because it eliminates the need to measure the sample's mass absorption coefficient. The derivation presented below is similar (but not identical) to that of Reynolds (1989) in that it avoids using reference intensity ratios (RIR) based on corundum, as defined by Chung (1974), and as applied by many authors utilizing powder diffraction file (PDF) data (*e.g.* Snyder and Bish, 1989). To avoid confusion, the notation introduced by Reynolds (1989), mineral intensity factor (MIF) is used. Our MIF is identical to RIR as redefined by Hubbard and Snyder (1988), except that ZnO rather than Al₂O₃ is used as the internal standard.

The wt.% of mineral X (%X) in a mixture *m* is proportional to the intensity of a reflection of this component (*I_x*) in the XRD pattern of the mixture (Klug and Alexander, 1974).

$$\%X = \frac{I_x \mu_m^*}{K_x} \quad (1)$$

where μ_m^* is the mass absorption coefficient of the mixture and K_x is a constant for a chosen reflection of mineral X, which depends on the structure, composition and density of mineral X, as well as on the experimental conditions of the XRD scan. This formula applies to thick and homogeneous samples.

Let us assume that a mixture *m* contains component X and a phase *S* chosen as an internal standard (spike). Then, a ratio of the content of mineral X (%X) and standard (%S) is

$$\frac{\%X}{\%S} = \frac{K_s \cdot I_x}{K_x \cdot I_s} \quad (2)$$

If the values of %X and %S are known and the intensities *I_x* and *I_s* of a chosen pair of reflections belonging to phases X and S are measured, then a so-called mineral intensity factor (MIF) of mineral X in a mixture with the standard can be calculated as

$$\text{MIF} = \frac{K_x}{K_s} = \frac{I_x \cdot \%S}{I_s \cdot \%X} \quad (3)$$

Thus, at a given set of experimental conditions, and for a chosen pair of reflections belonging to mineral X and standard S, MIF_X is a constant characteristic for mineral X. Its value does not depend on the concentration of mineral X and standard S in mixtures (if the sample is finely ground to eliminate microabsorption; Bish and Reynolds, 1989), on the mass absorption coefficient of the mix, or on the type or concentration of other phases in a given mixture. Thus, in general, equation 2 can be re-written as

$$\frac{\%X}{\%S} = \frac{I_x}{I_s \cdot \text{MIF}} \quad (4)$$

The MIF values for different minerals are determined by preparing mixtures with known amounts of the mineral of interest and the chosen internal standard. Then, to determine the unknown amount of mineral X (%X') in a sample, a known amount of the standard, *M_s*, is added to the sample. The weight percentages of mineral X (%X') and standard S (%S) in this mixture will be

$$\%X' = \frac{M_x \cdot 100}{M + M_s} \quad \text{and} \quad \%S = \frac{M_s \cdot 100}{M + M_s} \quad (5)$$

where *M_x* and *M* are the masses of mineral X and the sample to which standard is added, respectively.

The combination of equations 3, 4 and 5, remembering that %X = (*M_x*·100)/*M*, leads to

$$\frac{\%X'}{\%S} = \frac{M_x}{M_s} = \frac{\%X \cdot M}{M_s \cdot 100} = \frac{I_x}{(I_s \cdot \text{MIF})}$$

and the working equation

$$\%X = \frac{(I_x \cdot M_s \cdot 100)}{(I_s \cdot \text{MIF} \cdot M)} \quad (6)$$

where *I_x* and *I_s* are the intensities of reflections belonging to X and S in a mixture of a sample with the standard, and %X is the actual amount of the mineral in a sample without the standard. This approach allows for the direct quantitative measurement of each crys-

talline component of a sample, provided the appropriate MIF of the mineral of interest is available.

EXPERIMENTAL

Sample preparation

Sample splitting. In the initial stage of the study, samples were crushed in a mortar to pass through a 0.4 mm sieve and then several random splits were taken, ground, and diffraction data were collected under the same conditions. Qualitative inspection of the diffraction patterns showed that the relative proportion of various minerals was not the same using this splitting technique. Diffraction data identical within the measurement error were obtained when a louvered laboratory splitter was applied to split the crushed <0.4 mm samples. This method was then used as a standard procedure.

Sample grinding. Sample grinding is critical for both the precision (counting statistics) and accuracy (extinction, microabsorption, amorphization) of the quantitative analysis of bulk rocks (*cf.* Bish and Reynolds, 1989). Most laboratory mills currently in use are incapable of grinding to <20 μm (the maximum grain-size limit: Alexander and Klug, 1948), because their grinding process produces increasingly broader particle-size distributions, *i.e.* the coarse-size 'tail' remains. It was shown (O'Connor and Chang, 1986) that wet-grinding in a McCrone Micronizing Mill results in a narrow grainsize distribution. Such results were confirmed in the present study by SEM observations. Five minutes is the minimum time required to reduce the grain size of quartz or the shale components to <20 μm . Error in the integrated intensity of the quartz 3.34 Å reflection from five repeat measurements was <4%. Longer grinding times (up to 20 min) were tried and rejected. The longer times increase precision of measurement, but the quartz 3.34 Å reflection broadens progressively, and decreases in maximum intensity (up to 47%) and integrated intensity (up to 26%), as observed by many authors (amorphization, *e.g.* O'Connor and Chang, 1986). Thus 5 min of grinding was selected as the best compromise value.

Grinding was performed in methanol instead of water to accelerate drying of the ground sample and to avoid swelling of shale which could liberate individual clay crystals. In the shale, those crystals are naturally aggregated and these aggregates, if not broken by swelling, ensure random orientation. The use of water in spray-drying can liberate clay crystals without adverse effects because they ultimately end up on the surface of these spherical agglomerates (random orientation). In our technique, we do not use agglomeration and thus it is important to prevent the liberation of individual clay crystals which could orient during side-loading. A ratio of 3 g of sample to 4 ml of methanol was selected as the optimum proportion for the

slurry. Less sample in the mill results in measurable contamination of Al_2O_3 from the grinding rollers.

Internal standard addition and sample homogeneity. Zincite (ZnO) was selected as the internal standard (spike) because it provides stronger and more conveniently (although not perfectly) located reflections than corundum, Al_2O_3 , which is commonly used (Snyder and Bish, 1989). Several commercially available products were investigated and Baker[®] ZnO (catalog no. 1314-13-2) was found to be well crystallized (no XRD-detectable traces of amorphous material) and to provide very reproducible diffraction intensities (no large crystals). Additionally, the particle size of this ZnO (~1 μm mean size, checked by scanning electron microscopy) is sufficiently small to assume that microabsorption effects are negligible (Snyder and Bish, 1989). This product has diffraction characteristics comparable to National Bureau of Standards ZnO standard No. 674 (which is ten times more expensive).

Several homogenizing techniques were investigated and it was confirmed that adding ZnO prior to grinding in the McCrone mill (suggested by S. Hillier) produced fully reproducible results on splits from the same sample. Addition of 10 wt.% ZnO to the analyzed samples was selected as the optimum, based on the diffraction intensities.

Sample loading and clay particle orientation. Side-loading was found to be more satisfactory than front-loading for three reasons: reproducible density, more rigid specimens and lack of preferred orientation of clay particles. Front-loading circular 2.5 cm diameter holders, designed for use in a 40-position automatic sample changer, were modified to side-loading holders by milling out an appropriate side.

Side-loaded samples (see Moore and Reynolds, 1997, p. 220) can be densely (~0.6 g/cm^3) and reproducibly (2–4% of variation in density as opposed to 4–16% for front-loading) packed either by using a Vortexer shaker or by vigorously tapping the sample holder against the tabletop. The preparations packed by this technique are more rigid than front-loaded specimens, and thus they are resistant to deformation during movement in a sample changer. As a result, our side-loaded specimens (Figure 1b) produce much more reproducible XRD patterns than our front-loaded ones (Figure 1a).

Two tests were performed to address the problem of possible preferred orientation of clay particles. The first (Figure 2) compares diffraction data obtained from side-loaded preparations with that from splits of the same sample prepared by spray-freeze-drying. This technique is a variation (driving water off by sublimation instead of heating) of spray drying, which was shown to produce perfectly random orientation (Smith *et al.*, 1979; Hillier, 1999). The second test (Figure 3) investigated mixtures with varying proportions of

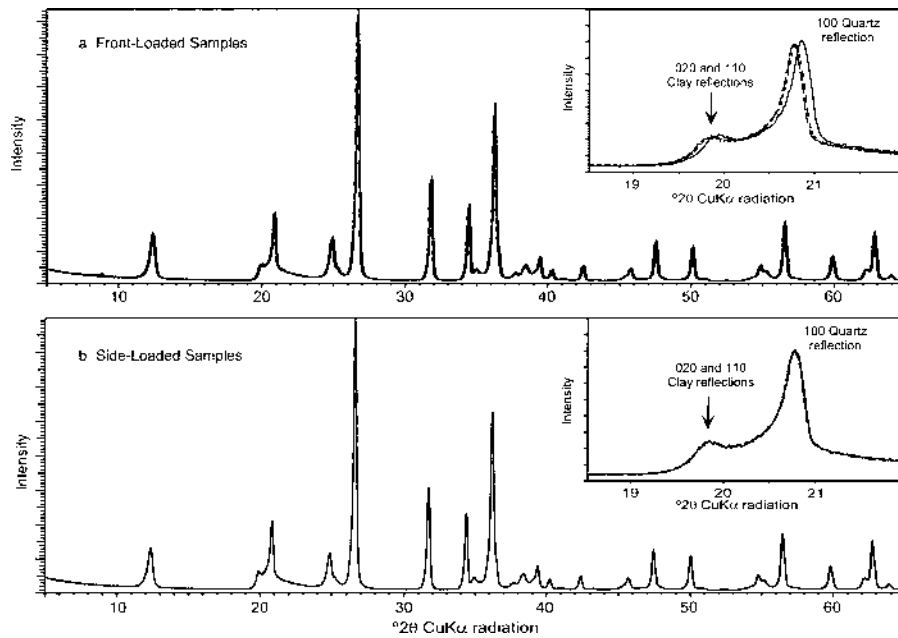


Figure 1. Sample loading test. Comparison of three front-loaded samples (a) and three side-loaded samples (b). Each curve represents the XRD scan from a separate aliquot of the same sample (mix of 40% quartz, 40% kaolinite and 20% ZnO by weight).

platy vs. isometric particles using different amounts of kaolinite and quartz.

For several clay/quartz/ZnO mixtures that were tested, the peak intensities did not show any systematic differences in $hk0$ vs. $00l$ reflection intensities, which

would be indicative of preferred orientation (Figure 2, insert B). The angle-dependant difference between the two patterns, apparent at low angles (Figure 2, insert A), results from different densities of the two specimens (Matulis and Taylor, 1992). The spray-freeze-

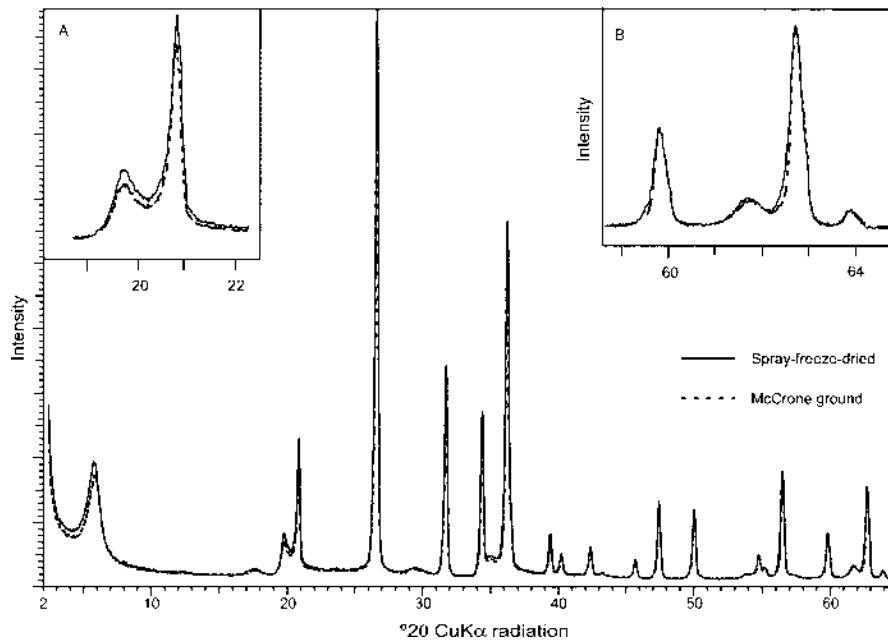


Figure 2. Sample orientation test. Comparison of the intensity of reflections between a sample ground in a McCrone mill and a spray-freeze-dried sample dried. The sample is composed of 20% ZnO, 40% quartz and 40% montmorillonite (Ca-saturated) by weight.

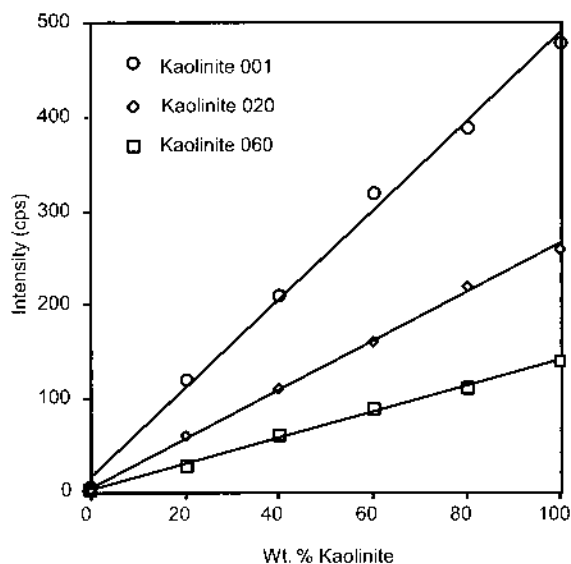


Figure 3. Sample orientation. Relationship between the content (wt.%) and the intensity of the kaolinite reflections 001, 020 and 060.

dried sample has intrinsically low density, which accounts for the observed differences.

In the second test, a linear relationship was found between wt.% kaolinite and the intensity of the kaolinite reflections 001, 020 and 060 (Figure 3). Such a linear dependence is only possible if there is a completely random orientation of the sample material. If a preferred orientation were present, kaolinite reflection intensity would be stronger when less disturbed by

smaller amounts of the isometric quartz grains and an exponential relationship in Figure 3 would result.

The two tests (Figures 2 and 3) are evidence that the applied preparation technique provides the required reproducibility and random orientation of particles necessary for QXRD.

XRD recording conditions

The XRD data were collected on a Siemens D-5000 diffractometer equipped with a 40-position sample holder, theta-theta goniometer, and a Kevex Peltier cooled silicon solid-state detector. CuK α radiation was used and the applied voltage was 50 kV with a 40 mA current. Based on five replicate analyses (Figure 4), counting 2 s per 0.02 $^{\circ}2\theta$ step was found to produce reproducible diffraction data for non-clay minerals in a reasonable registration time (e.g. 1140–1165 cps integrated intensity for quartz 100 reflection). Better statistics are needed for clay mineral quantification (060 region discussed in detail below) because the diagnostic reflections are weaker and broader than are those of non-clay minerals. Therefore, an additional scan at 5 s per 0.01 $^{\circ}2\theta$ step is required for the 59 $^{\circ}$ to 64 $^{\circ}2\theta$ region. These conditions were also used for recording patterns of standard mixtures used for MIF calculations.

For the initial tests, the goniometer settings applied were those that had been used previously in the Texaco laboratory for quantitative analysis: 2.0 mm divergence slit, 2.3 $^{\circ}$ incident beam Soller slit, and diffracted beam slits 2 mm, 0.2 mm plus 2.3 $^{\circ}$ Soller slit. Angle-dependent variations in peak intensity ratios for a giv-

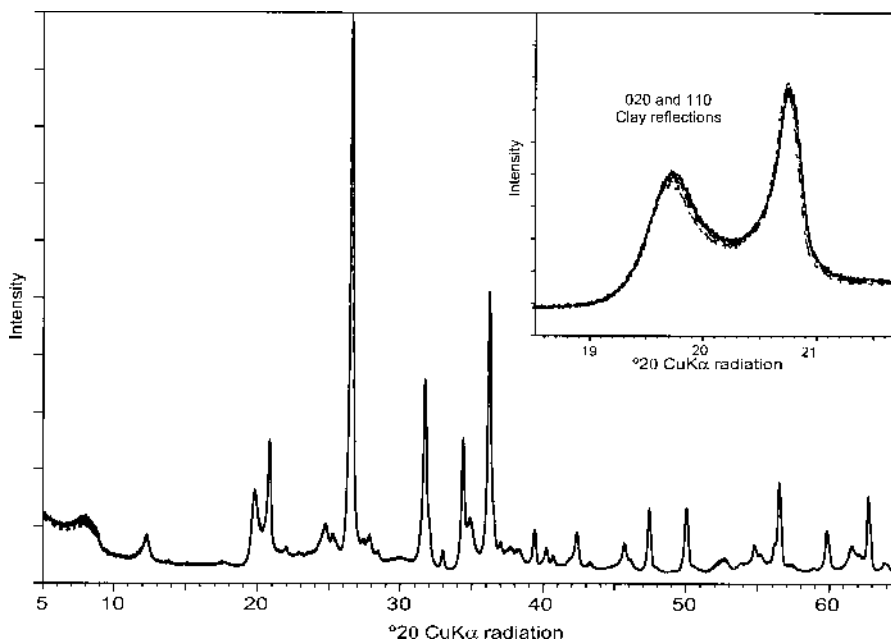


Figure 4. Comparison of diffraction data from five splits of the same shale sample.

en mineral analyzed alone and in mixtures were observed for these settings. The problem was solved by applying a 0.6 mm receiving slit and removing the diffracted-beam Soller slit. An additional advantage was a significant gain in absolute intensity, which is especially useful in analyzing minerals with low diffraction sensitivity or low concentration.

Zincite was found to be a better standard for monitoring machine drift (variation in peak intensity, shape and position, due to instrumental effects) than the Arkansas novaculite quartz plate supplied by the diffractometer manufacturers. The reproducibility of ZnO diffraction measurements from side-loaded powder preparations is better than measurements from novaculite slabs which contain many deep pores and occasional quartz crystals several tens of microns in diameter.

There is no diffracted beam intensity loss due to the sample length in the 2.5 cm diameter circular holders above $9.0^{\circ}2\theta$ under the experimental conditions used (Moore and Reynolds, 1997). Infinite sample thickness is assured at the high-angle end of the experimental range ($65^{\circ}2\theta$) if the preparation contains at least 30 mg/cm² of shale sample with a mass absorption coefficient, $\mu^* \approx 45\text{--}50$.

Selection and measurement of reference minerals

Potential reference samples were first analyzed by XRD to identify mineral contaminants. Samples, which were monomineral or contained small amounts of quantifiable contaminants, were selected for further work. The amount of a contaminant was estimated from chemical analysis by calculation of ideal structural formulae or from XRD data (quartz and albite in K-feldspars measured using MIFs of these minerals and not chemistry, because of Na for K substitution in K-feldspar). Major element chemical analyses were made by X-ray fluorescence (XRF) by X-ray Assay Laboratories (XRAL), Don Mills, Ontario, Canada. If available, several reference samples were used for each mineral. A summary of the reference minerals used and MIF values and associated reflections are shown in Table 1.

To ensure comparable grinding conditions, all non-clay minerals were mixed with high-defect kaolinite (poorly crystalline Georgia kaolinite, KGa-2, CMS source clay) in a 1:1 ratio and all clay minerals were mixed with quartz in a 1:1 ratio. To each standard mixture, 20 wt.% ZnO was added. Pure reference minerals were also run so they could be used in the peak decomposition routine (see below).

The MIF values were calculated for the diagnostic reflections (see below) using equation 3, and they are summarized in Table 1. They are calculated relative to the ZnO 100 reflection at 2.81 Å, the ZnO 002 reflection at 2.60 Å, and the ZnO 103 reflection at 1.47 Å. A MIF value averaged for all available samples is used

for all the minerals except dolomite and plagioclase feldspar. In practice, the albite MIF is used as the default for plagioclase feldspar, but others are available (Table 1a) if a different plagioclase is identified. A default standard MIF for dolomite is normally used unless independent evidence, generally petrographic, indicates an unusual form or chemistry such as high-temperature dolomite. Six orthoclase and five microcline standards were tested and, after correction for quartz and albite impurities, their calculated MIF values were similar (Table 1). Sanidine standard was not available. The MIF values are constantly being refined and are added to the database as additional samples of reference minerals become available.

Analytical reflection selection and treatment of XRD data for non-clay minerals

To the greatest extent possible, the diagnostic reflection chosen for each mineral should be significantly intense, free of coincidence with reflections from other common minerals, and stable with respect to peak intensity, shape and position (*i.e.* minimally affected by chemical and structural variations within a given mineral or mineral group). Because of possible coincidences with other common minerals, the diagnostic reflection chosen for a particular mineral may be different from one rock type to another. The diagnostic reflections chosen for quantitative analysis of shale rocks and carbonate rocks are shown in the diffraction patterns in Figure 5.

For this study, integrated intensity was measured using the commercial software program, EVA, which is contained in the Bruker/Siemens diffraction software package, Diffrac^{plus}. When no other reflection overlaps with the chosen reflection, a direct measurement can be made after establishing a linear background between two minima of the chosen reflection.

If there is a minor overlap of reflections, it is best to 'fit' the diagnostic reflection with the peak profile measured for the pure mineral, measured under the same experimental conditions (same shape). The XRD scan of the pure mineral is imported into the XRD scan of the sample and peak positions are made to coincide precisely by moving the imported peak along the $^{\circ}2\theta$ axis. The background level of the pure mineral is adjusted to that of the sample (which includes diffracted scattering from disordered clay structures and amorphous materials, producing *e.g.* a 'hump' in $19\text{--}34^{\circ}2\theta$ region). Then, the scan of the pure mineral is scaled so that the diagnostic reflections match one another (see Figure 6a). The integrated intensity of the mineral in the sample can then be measured directly from the scaled reflection of the pure mineral (Figure 6a). These direct and 'fitting' intensity measurements can also be performed using an Excel[™] macro program called Rock Jock, which is available from the authors.

Vol. 49, No. 6, 2001

Short title???

Table 1. MIF values used in this study and applied intensity corrections for overlapping reflections.

Mineral name	Reflection <i>d</i> value (Å)	# Reference minerals	Correction	MIF ₁₀₀	MIF ₀₀₂	MIF ₁₀₃
Barite (B)	101 (4.34)	1	none	0.12	0.20	0.23
Gypsum (G)	121 (4.28)	1	$Q_{101} \cdot \frac{Q_{100}^*}{Q_{101}^*}$	0.54	0.78	1.04
Quartz (Q)	100 (4.27)	3	$Ksp'_{002} \cdot \frac{Ksp_{201}^*}{Ksp_{002}^*}$	0.29	0.41	0.55
Anhydrite	101 (3.34)	1	none	1.39	1.99	2.65
	020 (3.49)		none	1.21	1.73	2.30
	202 (2.33)		none	0.19	0.27	0.35
K Feldspar (Ksp)	002 (3.25)	11	$H'_{200} \cdot \frac{H_{111}^*}{H_{200}^*}$	0.45	0.64	0.84
Plagioclase (Pg)	002 (3.20)	2	none	0.71	1.01	1.32
Calcite (C)	104 (3.03)	5	none	1.07	1.55	2.05
Mg Calcite	104 (2.99)	1	none	0.66	0.95	1.25
Ankerite	104 (2.91)	1	none	0.92	1.34	1.68
Dolomite (D)	104 (2.89)	2	none	0.82	1.18	1.56
	018 + 116 (1.79)		$G_{121} \cdot \frac{G_{262+321+181+260}^*}{G_{121}^*}$	0.30	0.44	0.58
Halite (H)	200 (2.81)	1	$S'_{018+116} \cdot \frac{S_{104}^*}{S_{018+116}^*} + Zn'_{103} \cdot \frac{Zn_{100}^*}{Zn_{103}^*} + B_{101} \cdot \frac{B_{211}^*}{B_{101}^*}$	1.11	1.60	2.11
Pyrite (P)	200 (2.72)	2	$B_{101} \cdot \frac{B_{002}^*}{B_{101}^*}$	0.94	1.42	1.72
Siderite (S)	018 + 116 (1.72)	1	$B_{101} \cdot \frac{B_{103+331+410}^*}{B_{101}^*} + Pg_{002} \cdot \frac{Pg_{062+472}^*}{Pg_{002}^*}$	0.46	0.66	0.87
Fe Chlorite (Ch)	060 (1.55–1.56)	2	$Q'_{100} \cdot \frac{Q_{211}^*}{Q_{100}^*} + D_{104} \cdot \frac{D_{122}^*}{D_{104}^*}$	0.09	0.13	0.18
Berthierine	060 (1.55–1.56)	1	$Q'_{100} \cdot \frac{Q_{211}^*}{Q_{100}^*} + D_{104} \cdot \frac{D_{122}^*}{D_{104}^*}$	0.12	0.17	0.22
Mg Chlorite (Ch)	060 (1.549)	5	$Q'_{100} \cdot \frac{Q_{211}^*}{Q_{100}^*} + D_{104} \cdot \frac{D_{122}^*}{D_{104}^*}$	0.15	0.22	0.29
Saponite	060	1	$Q'_{100} \cdot \frac{Q_{211}^*}{Q_{100}^*} + D_{104} \cdot \frac{D_{122}^*}{D_{104}^*}$	0.15	0.21	0.29
2:1 Fe clays	060 (1.51–1.52)	5	$B_{101} \cdot \frac{B_{251}^*}{B_{101}^*} + C_{104} \cdot \frac{C_{124+208+119}^*}{C_{104}^*}$	0.11	0.16	0.20
2:1 Al clays	060 (1.499–1.505)	10	$S'_{018+116} \cdot \frac{S_{122}^*}{S_{018+116}^*} + P'_{200} \cdot \frac{P_{023}^*}{P_{200}^*} + C_{104} \cdot \frac{C_{119}^*}{C_{104}^*}$	0.10	0.14	0.19
Kaolinite	060 (1.489)	5	none	0.09	0.13	0.17
ZnO (Zn)	103 (1.470)	1	$C_{104} \cdot \frac{C_{215}^*}{C_{104}^*}$	0.53	0.76	—
	002 (2.603)		none	0.69	—	1.31

Min X_{hkl} = measured integrated intensity with no correction, measured from the unknown sample spectrum.

Min X'_{hkl} = integrated intensity after correction has been applied, *i.e.* Min X'_{hkl} = (Min X_{hkl} - correction).

Min X_{hkl}^* = integrated intensity measured from a pure reference mineral XRD spectrum.

Ratios needed for corrections:

$$\begin{array}{llll}
 B_{002}^*/B_{101}^* = 3.581 & B_{103+331+410}^*/B_{101}^* = 0.769 & B_{211}^*/B_{101}^* = 3.057 & B_{251}^*/B_{101}^* = 1.746 \\
 C_{119}^*/C_{104}^* = 0.021 & C_{124+208+119}^*/C_{104}^* = 0.086 & C_{215}^*/C_{104}^* = 0.013 & D_{122}^*/D_{104}^* = 0.070 \\
 G_{262+321+181+260}^*/G_{121}^* = 0.339 & Ksp_{201}^*/Ksp_{040}^* = 0.237 & H_{111}^*/H_{200}^* = 0.097 & P_{023}^*/P_{200}^* = 0.210 \\
 Pg_{062+472}^*/Pg_{002}^* = 0.030 & Q_{101}^*/Q_{100}^* = 0.489 & Q_{100}^*/Q_{101}^* = 0.207 & S_{104}^*/S_{018+116}^* = 3.542 \\
 S_{122}^*/S_{018+116}^* = 0.184 & Zn_{100}^*/Zn_{103}^* = 1.89 & &
 \end{array}$$

Table 1a. MIF values for the plagioclase feldspars and for dolomite.

Mineral name	Reflection <i>d</i> value (Å)	# Reference minerals	Correction	MIF ₁₀₀	MIF ₀₀₂	MIF ₁₀₃
Albite	002 (3.20)	2	none	0.71	1.01	1.32
Oligoclase	002 (3.20)	3	none	0.66	0.95	1.25
Andesine	002 (3.20)	1	none	0.63	0.90	1.21
Labradorite	002 (3.20)	3	none	0.53	0.77	1.02
Bytownite	002 (3.20)	1	none	0.42	0.61	0.80
Anorthite	002 (3.20)	1	none	0.38	0.55	0.73
Dolomite-type 1	018 + 116 (1.79)	2	$G_{121} \cdot \frac{G_{262+321+181+260}^*}{G_{121}^*}$	0.30	0.44	0.58
Dolomite-type 2	018 + 116 (1.79)	15	$G_{121} \cdot \frac{G_{262+321+181+260}^*}{G_{121}^*}$	0.40	n.c.	n.c.

n.c.—not calculated.

If the overlap of different mineral reflections is significant, it is best to subtract the integrated intensity of one mineral from their intensity sum and obtain the other intensity by difference. This is done by measuring a non-overlapped reflection of the former mineral and applying the peak intensity ratio known from the reference sample diffraction scan to obtain the intensity to be subtracted. The diagnostic reflections are measured the same way both for the standard mixtures (calculation of MIF), and for unknown samples.

Standard peak decomposition techniques, based on fitting analytical functions, were also tried, but the technique of fitting the experimental peak profiles was found to be faster and more reliable. For each mineral and the internal standard, ZnO, a description is given in an Appendix (available on request from the Editor-

in-Chief or from the authors) which states the diagnostic reflection used along with the method of measuring integrated intensity. Diagnostic reflections and the corrections for overlapping reflections, if required, are also listed in Tables 1 and 1a.

Quantification of clay minerals

The 00*l* (basal) series of reflections was ruled out for use for quantification of clay minerals in whole-rock samples because of the high variability in intensity due to mixed layering and variable chemical composition. Such diffraction effects are well known for chlorites and the illite-smectite family (*e.g.* Moore and Reynolds, 1997), but in the course of this study, variations in basal intensities were also found to exist for kaolin minerals, which are free of

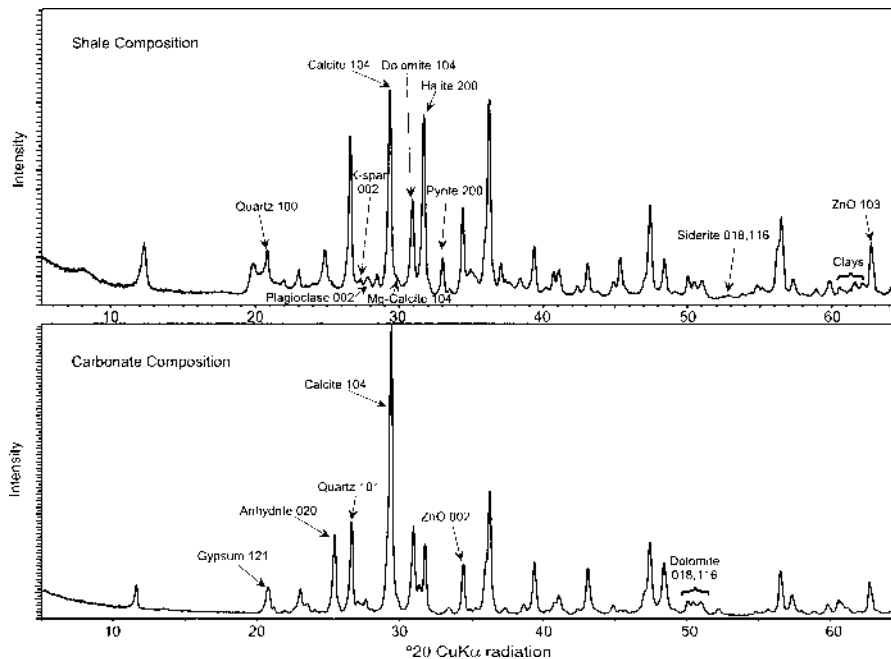


Figure 5. Diagnostic reflections used in the quantitative analysis method for shale and carbonate compositions.

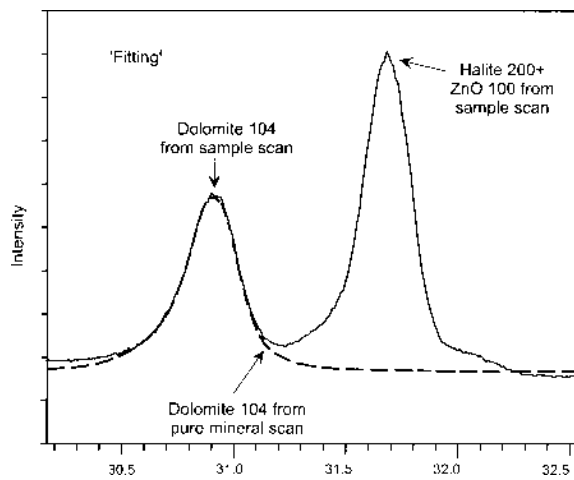


Figure 6. Measurement of integrated intensity by 'fitting' pure dolomite reflection (dashed).

mixed layering and have stable chemical composition and orientation.

The reflections having indices $h = 1 = 0$ are the best candidates for the analytical reflections, being relatively strong and least sensitive to polytypism and defects (*cf.* chapter 10 in Moore and Reynolds, 1997). The region containing 06 and 060 reflections was selected as optimum (as opposed to the 020 and 040 regions), because the reflections of different clays only partially overlap and their maxima can be distinguished readily (Figure 7). (Conventionally, $0k$ and $h0$ and $h00$ indices are used for the corresponding

reflections of clay minerals having turbostratic and 3D periodic structures, respectively. Both types of structures can often be found in shales. For some sheet silicates [phlogopite, chlorite, etc.] the 060 reflection is isolated, whereas for others [$1M$ and $2M$, Al-rich mica polytypes, kaolinite, berthierine, etc.] this reflection coincides with $33\bar{1}$. For simplicity, we use 060 notation.) The kaolinite 060 maximum is located at 1.489 Å; for aluminous dioctahedral 2:1 clays (montmorillonite, beidellite, illite-smectite, illite, and Al-rich mica) at 1.499–1.505 Å; for Fe-containing dioctahedral 2:1 clays (nontronite, glauconite, ferruginous illite and celadonite) at 1.51–1.52 Å; for trioctahedral Mg-rich chlorites at 1.549 Å; and for trioctahedral Fe-rich chlorite and berthierine at 1.55–1.56 Å. Thus, these five categories of clays can be quantified in this region, provided that peak decomposition can be performed successfully.

The chlorite 060 reflection is measured by subtracting the intensity contribution of the quartz 1.54 Å reflection from the measured total after scaling to the quartz reflection that is measured. For the remaining clays, the technique is based on 'fitting', as described in the previous paragraph. The background level of the standard is adjusted to that of the sample at $51^\circ 2\theta$ (the position with least mineral-related intensity). Fitting, followed by subtracting of the fitted peak is performed in a sequence, starting from the ZnO peak at 1.47 Å, and moving towards lower angles, as illustrated in Figure 8. The standard shapes of the illite-smectite family peaks differ

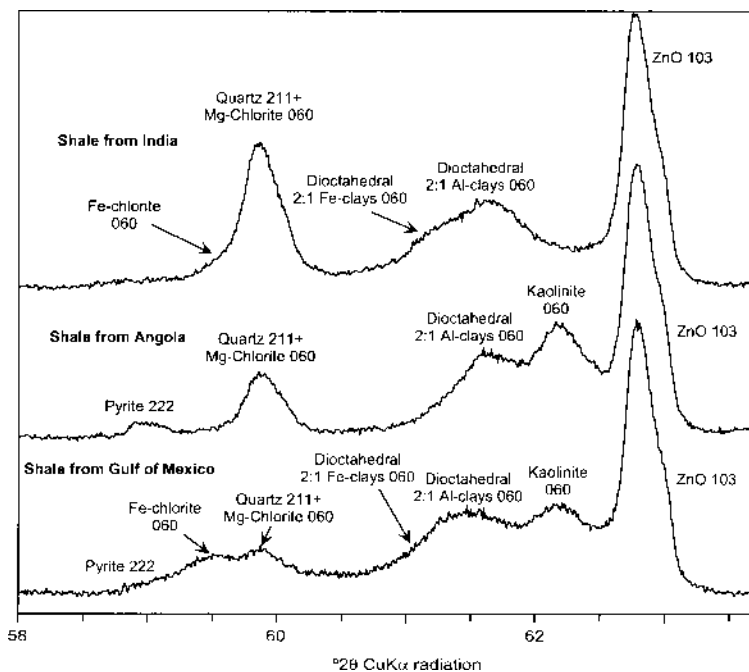


Figure 7. Clay 060 regions from three representative shales, illustrating the composition variation encountered in this study.

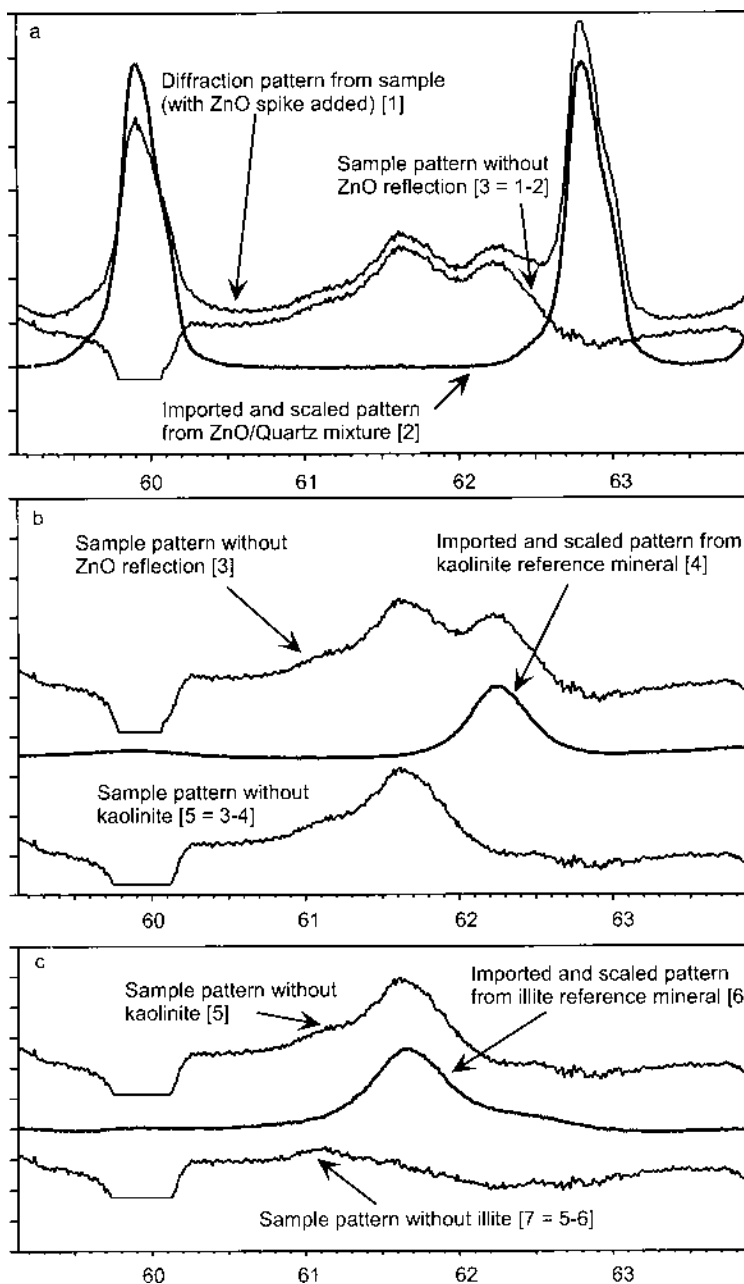


Figure 8. Procedure for decomposing the clay 060 diffraction data from a dioctahedral clay-rich shale (in parts b and c the curves are displaced along the y axis for clarity).

slightly depending on polytype (Figure 9), and so an appropriate standard has to be selected, based on the knowledge of the qualitative composition of the clay fraction. Most often, $1M_d$ illite or possibly smectite diffraction data are used. The 2:1 Fe-rich clay intensity is obtained as a residual after subtracting the 2:1 Al clay reflection. Details of the decomposition technique are presented in the Appendix (available from the Editor-in-Chief or authors on request).

Calculation of mineral composition

The mineral composition of samples can be calculated conveniently in a spreadsheet using equation 6. The dominant trioctahedral clay (berthierine, Fe-rich chlorite or Mg-rich chlorite) and the dominant Fe- or Al-rich 2:1 dioctahedral phase (smectite, $1M$, $1M_d$, or $2M_1$ illite or muscovite) have to be specified within the spreadsheet because their

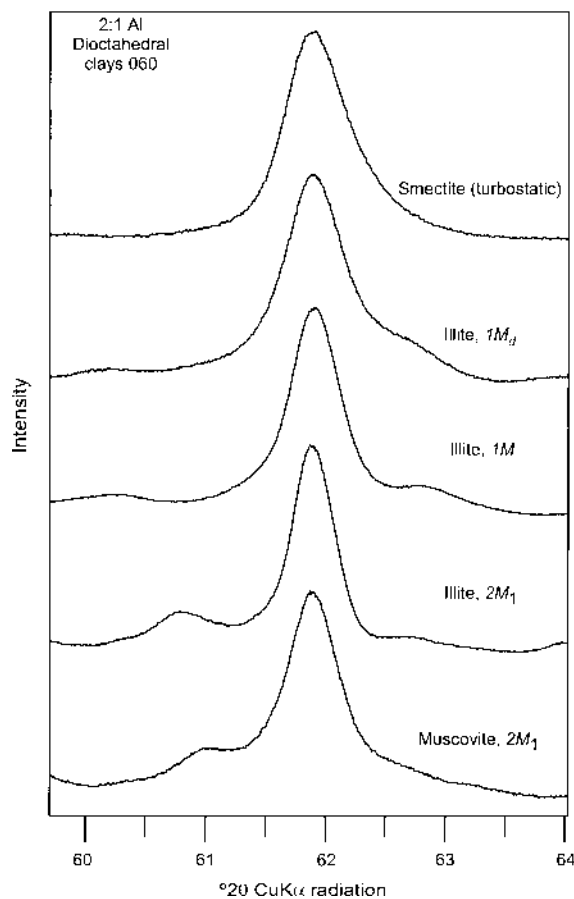


Figure 9. The 060 reflections from the 2:1 Al dioctahedral clays. The $1M$ and $2M_1$ samples have additional hkl reflections near the 060 reflection that produces a shoulder on the high-angle and low-angle sides, respectively.

MIFs are significantly different (Table 1). The 060 reflection for saponite occurs at $\sim 1.53 \text{ \AA}$, which is between those for berthierine/chlorite and dioctahedral Fe-rich 2:1 layer clays. If saponite is identified, its MIF has to be used (Table 1), which is similar to chlorite/berthierine, but different from the Fe-rich dioctahedral types.

The robustness of the entire analysis can be judged by how far the sum of measured minerals departs from 100%. It must be kept in mind that the presence of amorphous material, including organic matter, will reduce a total mineral sum. A more complete discussion of errors is presented below.

ANALYTICAL PERFORMANCE

Artificial rocks

Three artificial shale samples were created by thoroughly physically mixing selected amounts of reference minerals ($<0.4 \text{ mm}$ fractions). The proportions of various minerals were chosen to simulate the range of possible compositions encountered in natural ma-

terials. Splits were made of each mixture using a lowered laboratory splitter (see above) and submitted to three commercial vendor laboratories for quantitative analysis by XRD for comparison. The actual compositions of these artificial rocks are listed in Table 2, along with the mineral contents measured in the Texaco laboratory, using the method described here including grinding, and the compositions determined by the commercial vendors 1–3, who did the grinding themselves. Also shown in Table 2 are the results from a fourth commercial vendor (Vendor 4, Table 2) who analyzed the diffraction data obtained in the Texaco laboratory using Rietveld techniques. A detailed description of the analytical and preparation methods from these vendors was not provided. It is known that an internal standard was not used and that results were normalized to 100%. It is also known that vendors 1–3 obtained relative proportions of the clay minerals from oriented aggregate XRD analyses using a clay size-fraction. Clay proportions in the rock were calculated by partitioning the clay species accordingly from a ‘total clay’ intensity measurement in the bulk powder using the 020 110 composite reflection that is coincident in different dioctahedral clays.

The results by vendors 1–3 reflect their errors associated with sample preparation and diffraction data analysis, whereas those from Vendor 4 reflect our sample preparation error and their data analysis error. This vendor used the method of Rietveld refinement (non-clay minerals), combined with whole-pattern fitting (clay minerals). Our results reflect our sample preparation error, and our data analysis error, except the standard selection error (samples used to make the mixtures were used as standards).

A summary of the accuracy evaluation for each mineral analyzed in the artificial rocks using our technique is listed in Table 3, based on nine artificial shale samples (including those shown in Table 2) and three carbonate composition samples. The accuracy of these analyses is presented as standard error and as the mean difference from the actual value. The largest error is for the 2:1 Fe-rich clays, which is probably because it is a residual quantity and because there are strong interferences from non-clay minerals (*i.e.* calcite and others). For halite, the integrated intensity from at least two reflections is subtracted from that of the composite reflection (a third is possible if barite is present) and the resulting accuracy is quite low. There are different errors for quartz, calcite and dolomite between shale and carbonate compositions. Separate errors were calculated because of the different wt.% and different reflection overlaps of these minerals in the two rock types.

No systematic underestimation of the most abundant non-clay minerals (those with the strongest reflections) was observed, indicating no measurable error related to the detector dead time (Jenkins, 1989). This also

Table 2. Mineralogical analysis of three mixtures from Texaco using XRD (method described herein) and from four commercial vendors.

	Qtz	Ksp	Plag	Cal	Mg-Cal	Dol	Sid	Py	Kaol	2:1 Al clay	2:1 Fe clay	Fe Chl	Diop	Cumulative error from actual
<i>Sample A</i>														
Actual	25	5	5	5	0	0	0	0	15	20	20	5	0	
Texaco	26	4	3	5	0	0	0	0	16	19	22	5	0	8
Vendor 1	68	3	4	5	0	0	0	0	8	11*		0	0	87
Vendor 2	44	1	5	2	0.1	0	0.1	0	23	12*		11	0	68
Vendor 3	41	2	3	9	0	0	0	0	36	9*		0	0	82
Vendor 4	32	0	5	4	0	0	0	0	20	34	1	4	0	52
<i>Sample B</i>														
Actual	30	5	10	5	0	5	0	5	20	10	0	10	0	
Texaco	31	2	8	4	0	4	0	3	21	13	0	10	0	14
Vendor 1	56	0	7	3	0	6	0	14	12	2*		1	0	71
Vendor 2	34	1	8	3	0	6	0	4	24	2*		18	0	34
Vendor 3	52	2	3	13	0	0	0	2	24	5*		0	0	67
Vendor 4	34	0	7	4	0	4	0	6	20	15	0	6	4	28
<i>Sample C</i>														
Actual	30	10	5	5	5	5	10	0	10	15	0	5	0	
Texaco	30	8	4	5	5	4	10	0	10	16	0	5	0	5
Vendor 1	63	3	14	3	0	5	6	0	5	1*		0	0	84
Vendor 2	39	2	6	4	0	7	14	0.2	15	4*		10	0	51
Vendor 3	37	1	2	8	0	9	19	0	19	5*		0	0	64
Vendor 4	35	1	6	4	0	6	10	0	20	15	0	6	12	45

Qtz = quartz; Ksp = K-feldspar; Plag = plagioclase; Cal = calcite; Mg Cal = Mg calcite; Dol = dolomite; Sid = siderite; Py = pyrite; Kaol = kaolinite; Fe Chl = Fe-rich chlorite; Diop = diopside.

* Vendor did not differentiate between Al-rich and Fe-rich 2:1 clays.

implies that the MIF measurements are free of this error (probably because they were made on mixtures and not pure standards, so the intensities of the strongest reflections were not too high). There seems to be a systematic underestimation of pyrite content, which may be evidence of an error due to microabsorption (Reynolds, 1989). This error, if present, is so small that

it does not affect other components with high mass absorption coefficients (siderite, glauconite).

The errors of the method presented in this paper (Table 2) can be compared with the errors of the reported commercially available analyses, including the Rietveld analyses, only for quartz, calcite, and kaolinite. These three minerals have stable chemical com-

Table 3. Summary of accuracy evaluation for the method described herein.

	Shale composition			Carbonate composition		
	Range of mineral content (wt.%)	Standard error	Mean difference from actual (wt.%)	Range of mineral content (wt.%)	Standard error	Mean difference from actual (wt.%)
Quartz	3–35	0.1	0.7	5–10	0.1	0.2
K-feldspar	0.5–10	0.4	1.8			
Plagioclase	2.5–10	0.2	1.3			
Calcite	0–20	0.1	0.5	10–60	0.4	1.1
Mg-calcite	0–5	0.2	0.6			
Dolomite	0–13	0.1	0.5	15–60	0.2	0.4
Halite	0–5	0.5	1.6			
Pyrite	0–5	0.3	1.2			
Siderite	0–10	0.1	0.2			
Anhydrite	0			5–60	0.3	0.5
Gypsum	0			5–5	0.2	0.2
Kaolinite	7.5–60	0.3	0.8			
2:1 Al clay	0–60	0.4	1.4			
2:1 Fe clay	0–20	0.7	1.4			
Fe chlorite	0–5	0.2	0.4			
Mg chlorite	0	0.1	0.1			
Cumulative % difference:			12.4			2.4

¹ Evaluation based on nine shale samples of known composition, and three carbonate composition samples.

Vol. 49, No. 6, 2001

Short title???

Table 4. Results of analysis of 15 natural shale samples.

Mineral	Sample number														
	137	138	139	140	143	144	145	146	147	148	149	150	151	152	153
Quartz	27	23	8	14	15	19	30	2	31	25	12	14	19	45	7
K-feldspar	2	1	1	0	0	1	1	1	2	2	1	1	2	1	0.3
Plagioclase	5	2	1	3	3	4	1	0.5	3	2	1	1	1	2	0.4
Calcite	2	0	1	1	3	1	0	0.4	0.4	0	0.4	1	1	0.4	18
Mg calcite	1	2	0.4	1	1	1	1	0	1	2	1	1	1	0	0
Dolomite	2	0	0	0	1	1	0	0	0.4	0.3	0	0.3	0.3	14	0
Halite	0	0	0.1	0	9	0	0	0	0	0	0.2	0	0	1	1
Pyrite	0.3	2	2	0.2	2	0	0	1	2	5	2	2	1	0.3	0
Siderite	2	1	2	5	1	7	0	9	1	1	1	1	3	0	0
Barite	0	0	0	0	0	0	3	0	0	0	0	0	0	0	0
Gypsum	0	0	0	0	0	0	0	0	0	0	0	0	0	0	0
Ankerite	0	0	0	0	0	0	0.3	0	0	0	0	0	0.4	0	0
Total non-clay	40	31	16	24	35	36	37	14	41	37	19	21	28	64	27
Kaolinite	5	16	35	12	7	6	21	22	5	14	8	11	28	4	10
2:1 Al clay	44	42	45	43	51	34	38	27	33	47	47	53	21	32	34
2:1 Fe clay	7	7	0	3	3	16	0	24	14	0	16	14	10	0	24
Fe chlorite	0	0	0	18	0	10	0	0	0	0	0	0	11	0	0
Mg chlorite	2	4	5	0	2	0	0	0	3	0	0	0	0	2	3
Berthierine	0	0	0	0	0	0	7	13	0	1	5	1	0	0	0
Total clay	59	69	85	76	64	65	66	85	56	62	77	79	69	38	71
Sum	99	99	101	100	98	101	103	99	97	99	96	100	97	101	98

137 = offshore Gulf of Mexico, Gemini well

138 = offshore Angola, Espadarte well

139 = offshore Angola, unknown well

140 = onshore Oklahoma, Atoka well

143 = offshore Gulf of Mexico, Fuji well

144 = offshore Gulf of Mexico, west Delta 109 well

145 = Cretaceous outcrop, Colorado, Graneros Fm.

146 = offshore India, unknown well

147 = North Sea Miocene, unknown well

148 = offshore Nigeria, unknown well

149 = Central Graben, North Sea Oligocene, unknown well

150 = North Sea Oligocene, unknown well

151 = offshore Angola, Pennington well

152 = Cretaceous outcrop, Colorado, Skull Creek Fm.

153 = North Sea, Speeton Formation, unknown well

positions so the error of standard selection is negligible (negligible for kaolinite only if the 060 reflection is used, because this reflection is not affected by structural defects). This comparison is quite favorable for our technique, also with respect to Rietveld analysis, which performed best among the vendors.

Natural shales

This test was performed in order to obtain a qualitative evaluation for the collected MIF values using a range of different types of natural samples. Individual MIF values cannot be evaluated from natural rock samples, but the overall performance of the technique can be judged by the departure of sum from 100%. The 15 samples investigated, mostly from conventional core mudstones, are from different places around the world (Table 4). Such mudstone samples are commonly referred to as shales, although the term shale may not adhere to a strict petrological definition (Folk, 1980). The minerals that were identified by XRD included quartz, K-feldspar, plagioclase, calcite, magnesium calcite, dolomite, siderite, pyrite, halite, chlorite, berthierine, kaolinite and minerals of the illite-smectite group (Table 4).

The total sum of all minerals evaluated in the 15 natural samples range from 97% to 103% (Table 4).

These results are considered very good based on the cumulative error performance of 12.4% (Table 3).

CONCLUSIONS AND FURTHER PERSPECTIVES

The quantitative mineral analysis technique described in this paper allows us to measure accurately mineral compositions of rocks, including clay mineral content. The technique is particularly well suited to clay-rich samples, because diagnostic reflections of clays are weak compared to non-clay minerals. The advantage of this technique is that all minerals, including the clay groups, are quantified individually and directly as the wt.% of the bulk rock, without normalization and without a separate size separation and analysis from oriented preparations. The quality of the results can be judged by the departure of totals from 100%, provided the amorphous components are negligible or were quantified separately. In organic-rich rocks, or rocks containing amorphous metal oxides or hydroxides, this method can reveal the presence of such material by the departure of mineral content sum from 100%.

Using as the criterion the departure of totals from 100%, our results compare favorably with the technique of Smith *et al.* (1979), who used 001 clay reflections, spray drying and calculated μ^* from the ma-

for element chemical analysis. Our sample preparation technique is better than spray drying (Hiller, 1999), if a sample changer is used, because it produces rigid specimens, resistant to mechanical deformation that can occur during loading. The results of the artificial shale tests (Table 2) favor our technique over all the commercial ones that were tested, including the Rietveld-based approach.

Accuracy could perhaps be further increased and the time taken for analysis reduced if a more sophisticated method of integrated intensity measurements of overlapping reflections were applied. This aspect is particularly important for clays because broad reflections make integrated intensities difficult to measure.

There may be a more suitable internal standard than ZnO that meets size and crystallinity criteria, but that has more conveniently located reflections. Such a standard would increase the clay analysis accuracy by avoiding the kaolinite 1.49 Å/ ZnO 1.47 Å partial overlap. If another internal standard were to be used, all MIF values measured with ZnO can be recalculated. Additionally, the present MIF database should be expanded for minerals with a wide range of chemical compositions, in particular dolomite, Mg-calcite and siderite.

The individual clay mineral groups that are quantified with this technique include: kaolinite, 2:1 aluminous clays (smectite + illite-smectite + illite + Al-rich mica), 2:1 Fe-rich clays (nontronite + glauconite + Fe-rich illite + celadonite), Mg-rich chlorite and Fe-rich chlorite + chamosite + biotite. Such grouping of clay species is different from the identification readily available from 001 reflections and advantageous for quantifying relationships between clays of different origin (*e.g.* those that are Fe-rich and Al-rich). Such clay quantification is also important for geological engineering concerns. Information on the detailed mixed-layer structure of the clay component is not possible by this type of analysis and has to be obtained separately. The most reliable method is a detailed computer simulation of the diffraction data obtained from oriented preparations (*e.g.* Drits *et al.*, 1997; Lindgreen *et al.*, 2000; McCarty *et al.*, 2000).

Table 4 presents the mineral composition of shales, typical for petroleum basins worldwide. These data show that there is a broad compositional range in these rocks. The non-clay content of such rocks varies from 14 to 64%, mostly due to variation in quartz content (2 to 45%, respectively). Low-quartz rocks are either kaolinite-rich (up to 35%; redeposited laterites or vertisols) or are rich in authigenic 2:1 Fe clays. In high-quartz rocks, 2:1 Al clays are dominant (typically 30–50% of the bulk rock). The content of Fe-rich authigenic clays (2:1 Fe clay plus Fe-chlorite plus berthierine) varies widely from 0 to 37%. The remaining minerals occur in subordinate quantities.

ACKNOWLEDGEMENTS

The collection of mineral standards at Texaco was supplemented by samples supplied by colleagues from different institutions: chlorites (Steve Hillier and Jeff Walker), berthierine (Dewey Moore), low-temperature albite and K-feldspar (Richard Hay). E-mail discussions with Steve Hillier were very helpful. This work would not have been possible without tremendous help from Andrew Thomas, Kymberli Correll, Jessy Jones and Amy Blackwell. Critical reviews by David Bish and anonymous reviewers were very helpful in improving the presentation of our work.

REFERENCES

- Alexander, L. and Klug, H.P. (1948) Basic aspects of X-ray absorption in quantitative analysis of powder mixtures. *Analytical Chemistry*, **20**, 886–889.
- Batchelder, M. and Cressey, G. (1998) Rapid, accurate phase quantification of clay-bearing samples using a position-sensitive X-ray detector. *Clays and Clay Minerals*, **46**, 183–194.
- Bish, D.L. and Howard, S.A. (1988) Quantitative phase analysis using the Rietveld method. *Journal of Applied Crystallography*, **21**, 86–91.
- Bish, D.L. and Reynolds, R.C., Jr. (1989) Sample preparation for X-ray diffraction. Pp. 73–100 in: *Modern Powder Diffraction* (D.J. Bish and J.E. Post, editors). Reviews in Mineralogy, **20**. Mineralogical Society of America, Washington, D.C.
- Brindley, G.W. (1980) Quantitative analysis of clay mixtures. Pp. 411–438 in: *Crystal Structures of Clay Minerals and their X-ray Identification* (G.W. Brindley and G. Brown, editors). Mineralogical Society, London. Monograph 5.
- Chung, F.H. (1974) Quantitative interpretation of X-ray diffraction patterns of mixtures. I. Matrix flushing method for quantitative multicomponent analysis. *Journal of Applied Crystallography*, **7**, 519–525.
- Drits, V.A., Sakharov, B.A., Lindgreen, H. and Salyn, A. (1997) Sequential structure transformation of illite-smectite-vermiculite during diagenesis of Upper Jurassic shales from the North Sea and Denmark. *Clay Minerals*, **32**, 351–371.
- Folk, R.L. (1980) *Petrology of Sedimentary Rocks*. Hemphill Publishing Co., Austin, Texas, 184 pp.
- Hillier, S. (1999) Use of an air-brush to spray dry samples for X-ray powder diffraction. *Clay Minerals*, **34**, 127–135.
- Hubbard, C.R. and Snyder, R.L. (1988) RIR—measurement and use in quantitative XRD. *Powder Diffraction*, **3**, 74–77.
- Jenkins, R. (1989) Experimental procedures. Pp. 47–20 in: *Modern Powder Diffraction* (D.J. Bish and J.E. Post., editors). Reviews in Mineralogy, **20**. Mineralogical Society of America, Washington, D.C.
- Klug, H.P. and Alexander, L.E. (1974) *X-ray Diffraction Procedures*. J. Wiley & Sons, New York, 966 pp.
- Lindgreen, H., Drits, V.A., Sakharov, B.A., Salyn, A.L., Wrang, P. and Dainyak, L.G. (2000) Illite-smectite structural changes during metamorphism in black Cambrian Alum shales from the Baltic area. *American Mineralogist*, **85**, 1223–1238.
- Lynch, F.L. (1997) Frio shale mineralogy and the stoichiometry of the smectite-to-illite reaction: the most important reaction in clastic sedimentary diagenesis. *Clays and Clay Minerals*, **45**, 618–631.
- Matulis, C.E. and Taylor, J.C. (1992) Intensity calibration curves for Bragg-Brentano X-ray diffractometers. *Powder Diffraction*, **7**, 89–94.

Vol. 49, No. 6, 2001

Short title???

- McCarty, D.K., Hsieh, J.C.C., Drits, V.A. and Środoń, J. (2000) The mineralogy of mudstones: clay mineral heterogeneity. *GSA, Abstracts With Programs*, **32(7)**, p. 321.
- McManus, D.A. (1991) Suggestions for authors whose manuscripts include quantitative clay mineral analysis by X-ray diffraction. *Marine Geology*, **98**, 1–5.
- Moore, D.M. and Reynolds, R.C., Jr. (1997) *X-ray Diffraction and the Identification and Analysis of Clay Minerals*. Oxford University Press, Oxford, 378 pp.
- Mossman, M.H., Freas, D.H. and Bailey, S.W. (1967) Orienting internal standard method for clay mineral X-ray analysis. *Clays and Clay Minerals*, **15**, 441–453.
- O'Connor, B.H. and Chang, W.J. (1986) The amorphous character and particle size distribution of powders produced with the micronizing mill for quantitative X-ray powder diffractometry. *X-ray Spectrometry*, **15**, 267–270.
- Reynolds, R.C., Jr. (1989) Principles and techniques of quantitative analysis of clay minerals by X-ray powder diffraction. Pp. 4–36 in: *Quantitative Mineral Analysis of Clays* (D.R. Pevear and F.A. Mumpton, editors). CMS Workshop Lectures **1**. The Clay Minerals Society, Bloomington, Indiana.
- Smith, D.K., Johnson, G.G., Jr., Scheible, W., Wims, A.M., Johnson J.L. and Ullmann G. (1987) Quantitative X-ray powder diffraction method using the full diffraction pattern. *Powder Diffraction*, **2**, 73–77.
- Smith, S.T., Snyder, S.L. and Brownell, W.E. (1979) Quantitative phase analysis of Devonian shales by computer controlled X-ray diffraction of spray dried samples. *Advanced X-ray Analysis*, **22**, 181–191.
- Snyder, R.L. and Bish, D.L. (1989) Quantitative analysis. Pp. 101–144 in: *Modern Powder Diffraction* (D.J. Bish and J.E. Post., editors). Reviews in Mineralogy, **20**. Mineralogical Society of America, Washington, D.C.
- Taylor, J.C. (1991) Computer programs for standardless quantitative analysis of minerals using the full powder diffraction profile. *Powder Diffraction*, **6**, 2–9.
- Taylor, J.C. and Matulis, C.E. (1994) A new method for Rietveld clay analysis. Part I. Use of a universal measured standard profile for Rietveld quantification of montmorillonites. *Powder Diffraction*, **9**, 119–123.
- Ward, C.R., Taylor, J.C. and Cohen, D.R. (1999) Quantitative mineralogy of sandstones by X-ray diffractometry and normative analysis. *Journal of Sedimentary Research*, **69**, 1050–1062.
- E-mail of corresponding author: ndsrodon@cyf-kr.edu.pl
(Received 14 December 2000; revised 6 April 2001; Ms. 506).